

# PHASE ESTIMATION ALGORITHM FOR FREQUENCY HOPPED BINARY PSK AND DPSK WAVEFORMS WITH SMALL NUMBER OF REFERENCE SYMBOLS

Benjamin R. Wiederholt  
The MITRE Corporation  
Bedford, MA

and  
Mario A. Blanco  
The MITRE Corporation  
Bedford, MA

Approved for Public Release; Distribution Unlimited  
Case #05-0778

## ABSTRACT

*In military satellite communication systems that use frequency hopped waveforms, it is difficult to coherently detect phase shift keying (PSK) (binary or M-ary) signals unless many reference symbols are used to aid with phase estimation of the received signal. For this reason, many systems use differential phase modulations, such as differential phase shift keying (DPSK), which can be detected noncoherently without the use of phase information. However, the use of DPSK over PSK results in reduced power efficiency. This paper presents a novel approach to phase estimation that provides improved power efficiency through coherent detection of phase modulated signals (with and without differential encoding) using few reference symbols. More specifically, the algorithm presented herein uses signal processing techniques to estimate the phase of each hop by using both reference and information symbols in a hop. This paper focuses on binary PSK and DPSK waveforms where data is transmitted in blocks with only one or two reference symbols per block. The performance of this algorithm was evaluated for the case of additive white Gaussian noise (AWGN) and Rayleigh fading channels via Monte Carlo simulations. At bit error rates (BER) of interest, the results indicate that, depending on the environment and modulation used, performance gains of up to 3 dB were realized when hops contain as few as two reference symbols. The results also show that coherent detection of binary phase shifting keying (BPSK) and DPSK modulated waveforms containing one reference symbol per hop performed more efficiently than noncoherent detection in all channels considered*

## 1. INTRODUCTION

Frequency hopped waveforms in military satellite communication systems are characterized by the number of reference and information symbols contained in each transmitted block of data. When these blocks of data hop from one carrier frequency to the next, the unknown phase introduced by the channel also changes. To efficiently detect the received signal using coherent methods, phase modulated waveforms utilize the known reference symbols to estimate the phase of each hop. In order for these waveforms to perform near theoretical coherent detection, hops

must contain a sufficiently large number of reference symbols. Since phase information cannot be accurately determined from waveforms containing few reference symbols, systems typically overcome the phase ambiguity by employing power inefficient differential phase modulations that can be noncoherently detected. As a result, depending on the environment and modulation used, such systems can suffer power losses of up to 3 dB.

This paper presents two phase estimation algorithms that provide improved power efficiency through coherent detection of binary phase modulated waveforms containing a small number of reference symbols. Both algorithms use signal processing techniques to estimate the phase of each hop using the reference and information symbols. The algorithms performance was evaluated through Monte Carlo simulations of BPSK and DPSK waveforms in AWGN and Rayleigh fading channels. Within each modulation and channel, hops containing only one and two reference symbols were considered. The advantage of the phase estimation algorithms was quantified by comparing the performance of coherent BPSK and DPSK detection to noncoherent DPSK detection. This paper concludes by demonstrating that the algorithms presented can be extended to estimate the phase of quadrature phase shift keying (QPSK) and eight-phase shift keying (8PSK) modulated waveforms.

## 2. ALGORITHM DESCRIPTION

The algorithms presented here overcome the limitations of phase modulated waveforms containing few reference symbols by using a unique approach to estimate the phase of each hop. The foundation of each algorithm is a simple squaring technique which modifies all symbols within a hop so that reference and information symbols can be used to estimate the phase. By making use of the inherent properties of differential decoding, this technique alone produces estimates which support coherent DPSK detection. However, additional corrective measures using knowledge from the reference symbols are required to estimate the phase of BPSK modulated waveforms.

### 2.1 DPSK Algorithm

Figure 1 illustrates the DPSK phase estimation algorithm block diagram.

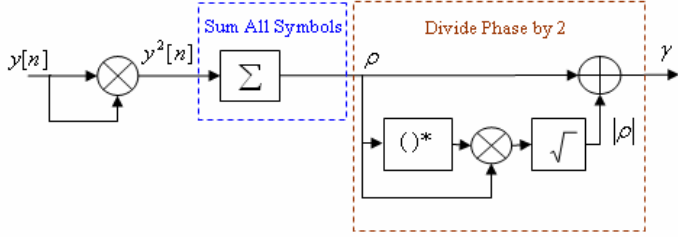


Figure 1: Block Diagram for DPSK Phase Estimation Algorithm

To demonstrate the sequence of this algorithm, the base-band signal received at the input of Figure 1 is shown as

$$y[n] = x[n]\kappa[n]e^{j\theta'[n]} \quad (1)$$

where  $x[n]$  is the differentially encoded data ( $x[n] = \pm 1$ ) and  $\kappa[n]$  and  $\theta'[n]$  are the noise corrupted amplitude and phase rotation of each symbol.

The first step of the algorithm is to square the input  $y[n]$  to remove the data component so that all symbols represent one phase. As a result, the squaring produces

$$y^2[n] = \kappa^2[n]e^{j2\theta'[n]} \quad (2)$$

where the  $180^\circ$  phase shift is removed at the expense of each symbol being shifted to  $2\theta'[n]$ . The squaring also loses the location of the true phase offset due to the modulo- $2\pi$  addition. With all samples representing one phase offset, the average rotation of  $L$  symbols in a hop is determined by

$$\begin{aligned} \rho &= \sum_{n=1}^L y^2[n] \\ &= |\rho|e^{j2\hat{\theta}} \end{aligned} \quad (3)$$

Since the summation determines the average rotation of twice the desired phase,  $\rho$  is corrected by dividing the phase by two. The phase division is performed by adding a vector of equal magnitude and zero phase. The proof of this division technique is shown as

$$\begin{aligned} \gamma &= \rho + |\rho| = |\rho|e^{j2\hat{\theta}} + |\rho|e^{j0} \\ &= 2\cos(\hat{\theta})|\rho|e^{j\hat{\theta}} \end{aligned} \quad (4)$$

Since the rotation of  $\gamma$  is only of interest, the magnitude  $2\cos(\hat{\theta})|\rho|$  is ignored and the phase estimate becomes  $\hat{\theta}$ .

The properties of differential decoding allow DPSK modulated waveforms to be coherently detected using either the true offset or a  $180^\circ$  shift from the offset. Consequently, this algorithm is limited to coherent DPSK detection since the true offset is lost by the squaring in (2).

## 2.2 BPSK Algorithm

The BPSK algorithm employs the same squaring and phase division approach used by the DPSK algorithm to find the average rotation of all symbols in a hop. However, since BPSK modulated waveforms are not differentially encoded, the true phase offset must be determined through an additional phase correction process. The basic structure of this algorithm is shown in Figure 2.

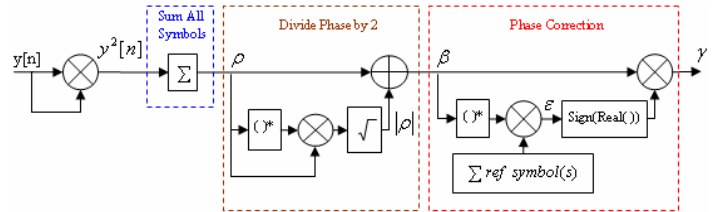


Figure 2: Block Diagram for BPSK Phase Estimation Algorithm

For illustrative purposes, the phase estimate in (4) is shown as

$$\beta = \pm e^{j\hat{\theta}} \quad (5)$$

where the  $\pm$  denotes the  $180^\circ$  phase ambiguity that results from the squaring in (2).

Since the reference symbol(s) represent the true offset, the phase ambiguity is corrected using the average rotation of the reference symbols. The first step in correcting the phase is to find the phase error of  $\beta$  by

$$\varepsilon = \beta^* \left( \sum \text{ref symbol}(s) \right) \quad (6)$$

The hard decision to shift  $\beta$  by  $180^\circ$  or  $0^\circ$  is made based on the angle of the phase error. This decision becomes

$$\begin{aligned} \text{if } \varepsilon > -90^\circ \text{ and } \varepsilon < 90^\circ \Rightarrow \text{sign}(\text{Re}(\varepsilon)) = 1 \\ \gamma = (1)\beta \end{aligned} \quad (7)$$

$$\begin{aligned} \text{if } \varepsilon > 90^\circ \text{ or } \varepsilon < -90^\circ \Rightarrow \text{sign}(\text{Re}(\varepsilon)) = -1 \\ \gamma = (-1)\beta \end{aligned} \quad (8)$$

This correction recovers the information lost by the squaring in (2) and produces an estimate  $\gamma$  which is near the true offset.

## 2. WAVEFORM MODEL

The performance of the phase estimation algorithm was evaluated through Monte Carl simulations of BPSK and DPSK waveforms in AWGN, fast Rayleigh fading, and slow (flat) Rayleigh fading channels. The simulations were developed using the discrete baseband receiver model shown in Figure 3.

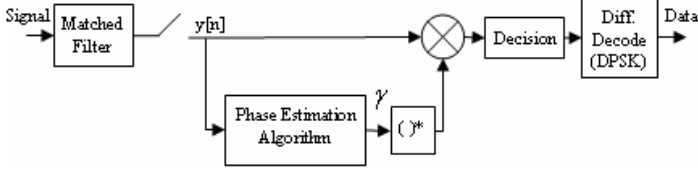


Figure 3: BPSK and DPSK Baseband Receiver with Phase Estimation Algorithm

The received signal with L symbols per hop was modeled at the output of matched filter as

$$y[n] = \alpha x[n] \sqrt{\frac{2E_b}{N_o}} e^{j\theta} + N(0,1) \quad n = 1, 2, 3 \dots L \quad (9)$$

where  $\alpha$  is the amplitude variation dictated by the channel and  $x[n]$  is the binary data or differentially encoded binary data ( $x[n] = \pm 1$ ) [1]. The model uniformly generated the unknown phase  $\theta$  and assumed it remains constant over all L symbols. The Gaussian noise was normalized with  $E(N) = 0$  and  $Var(N) = 1$  so that the signal to noise ratio (SNR) could be varied directly.

The AWGN channel was modeled assuming the signal was only corrupted by the spectral noise. Therefore, the amplitude variation in (9) was set to

$$\alpha = 1 \quad (10)$$

By contrast, the two Rayleigh fading channels were modeled assuming the signal corruption was due to amplitude degradation as well as additive noise. For these channels,  $\alpha$  became a Rayleigh distributed random variable with a predetermined mean and variance so that the model simulated an average SNR of  $\frac{E_b}{N_o}$ . This condition was satisfied

when  $E(\alpha) = \sqrt{\frac{\pi}{4}}$  and  $Var(\alpha) = 1 - \frac{\pi}{4}$  so that when moved inside the square root,  $\alpha$  became an exponential distribution with  $E(\alpha^2) = 1$  [2].

Within this Rayleigh fading model, two fading examples were considered. The first case was fast Rayleigh fading where  $\alpha$  varied from symbol-to-symbol. As a result, a Rayleigh distributed vector of length L was generated by

$$\alpha[n] = \sqrt{-\ln(1-u[n])} \quad n = 1, 2, 3 \dots L \quad (11)$$

where u represents a random variable uniformly distributed over (0,1).

The other case considered was slow (flat) Rayleigh fading where the amplitude variation was equally affected by all frequency components. This channel was modeled by generating a single  $\alpha$  for each hop by

$$\alpha = \sqrt{-\ln(1-u)} \quad (12)$$

The received signal in (9) was passed to the phase estimation algorithm where the phase of the hop was estimated using all L symbols. Using the phase estimate, the output of the matched filter was coherently detected and hard decisions were made as

$$\hat{x}[n] = \text{Re}\{y[n]\gamma^*\} \stackrel{\leq}{>} 0 \quad (13)$$

In the case of the DPSK waveform, the coherently detected data was differentially decoded.

## 3. PERFORMANCE RESULTS

The channels discussed in this paper demonstrate three different environments which affect phase estimation in satellite communications. The simulations of the waveform and channel models presented in Section 2 provide a measure of the phase estimation algorithm performance. The advantage of phase estimation was quantified by comparing the algorithm BER versus SNR waterfall curves to the noncoherent DPSK waterfall curves at  $BER = 10^{-2}$ . The difference between these curves signifies the power savings achieved through coherent detection using phase estimation.

The algorithms ability to estimate the phase of each hop using a small number of reference symbols is shown here through simulation results of two different hop structures for each channel and modulation. The first structure considered had one reference symbol at the beginning of each hop followed by eight information symbols. The other contained two reference symbols at the beginning followed by sixteen information symbols.

### 3.1 AWGN Channel

Figure 4 demonstrates the performance of the BPSK and DPSK algorithms in the AWGN channel when each hop contained only one reference symbol. These results show that the DPSK and BPSK algorithms performed similarly. At  $BER = 10^{-2}$ , both waveforms performed 0.68 dB more efficiently than noncoherent DPSK detection. These gains illustrate that the DPSK algorithm approached near theoretical performance while the BPSK algorithm under-achieved by comparison. Using only one reference symbol to perform phase correction, the BPSK algorithm was

unable to achieve large performance gains due to bursty errors produced by estimates with phase errors near  $\pm 180^\circ$ .

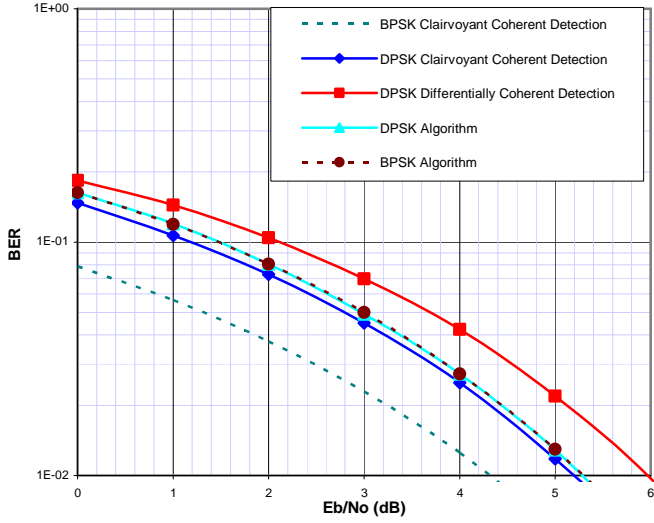


Figure 4: AWGN channel - 1 Reference Symbol and 8 Information Symbols

To demonstrate the influence of the reference symbols, the performance of BPSK and DPSK waveforms with two reference symbols and sixteen information symbols in each hop are shown in Figure 5. In comparison to the first hop structure considered, these results show that the BPSK algorithm performed quite differently than the DPSK algorithm. The DPSK algorithm outperformed noncoherent DPSK detection by 0.71 dB while the BPSK algorithm realized a 1.5 dB improvement at  $BER=10^{-2}$ . The relatively large performance advantage of the BPSK algorithm was attributed to the improved phase correction using two known reference symbols. More specifically, the two reference symbols accurately resolved the  $180^\circ$  phase ambiguity that results from the squaring operation in (2).

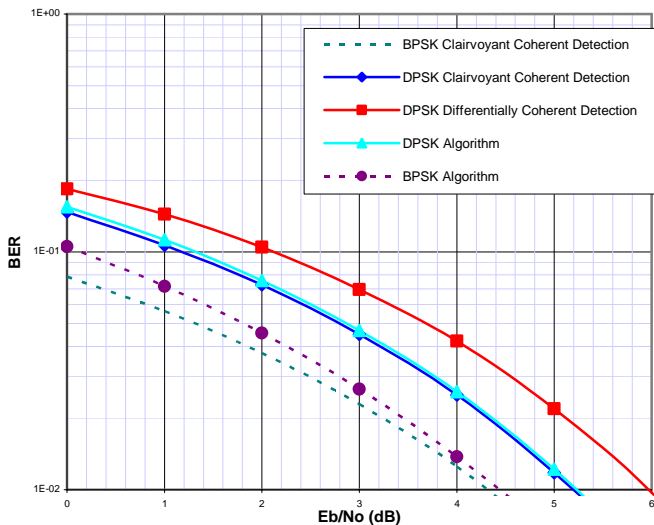


Figure 5: AWGN Channel - 2 Reference Symbols and 16 Information Symbols

### 3.2 Fast Rayleigh Fading Channel

The fast Rayleigh fading channel is an alternative environment in which waveform and algorithm performance is affected. The performance of the BPSK and DPSK algorithms in this channel are shown in Figure 6. These results demonstrate that at  $BER=10^{-2}$ , the algorithms experienced a small power improvement of 0.10 dB over noncoherent DPSK detection when hops contain one reference symbol. In this channel, the DPSK algorithm was limited to small gains since theoretical coherent DPSK detection and noncoherent DPSK detection converged at high SNR. However, as seen in the AWGN channel, the BPSK algorithm underperformed when phase correction was performed with only one reference symbol.

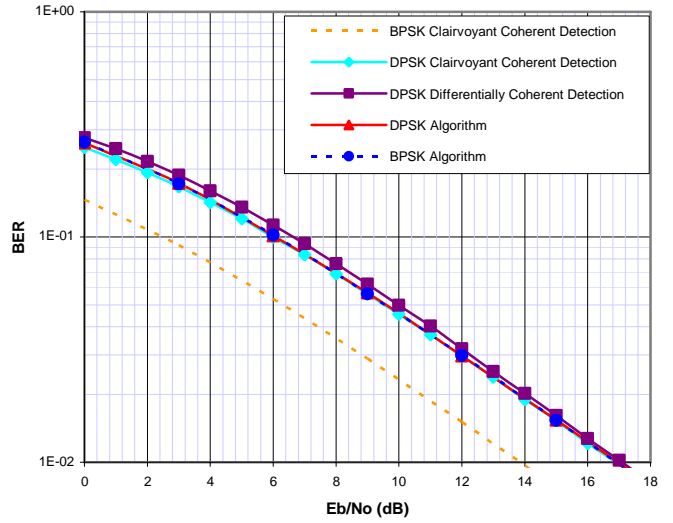


Figure 6: Fast Fading Channel - 1 Reference Symbol and 8 Information Symbols

Even though the DPSK algorithm achieved near theoretical performance with only one reference symbol per hop, adding an additional reference symbol aided the performance of the BPSK algorithm. The results in Figure 7 show that when hops contain two reference symbols, the BPSK algorithm performed 3.05 dB better than noncoherent detection. Again, the improved performance was credited to reducing the phase errors near  $\pm 180^\circ$  by using two reference symbols to perform the phase correction.

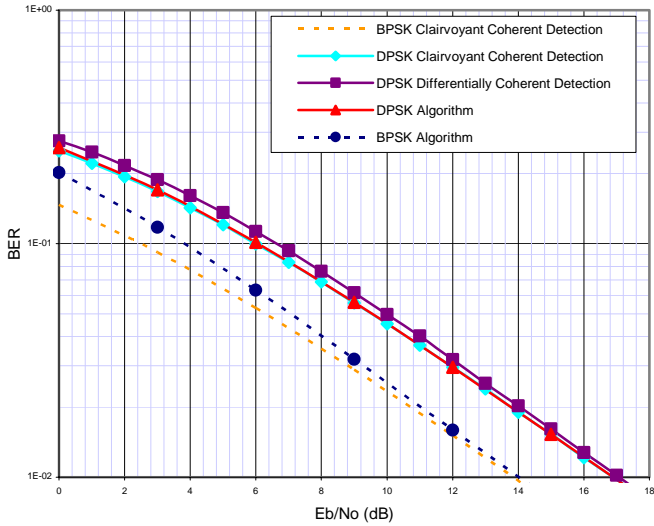


Figure 7: Fast Fading Channel - 2 Reference Symbols and 16 Information Symbols

### 3.3 Slow (Flat) Rayleigh Fading Channel

In comparison to the fast fading channel, the slow fading channel results in Figure 8 show that theoretical coherent and noncoherent DPSK detection maintained a constant difference over the entire range of SNR. As a result, the DPSK and BPSK algorithms with one reference symbol per hop achieved a sizeable 0.55 dB advantage over noncoherent detection. However, the performance of both algorithms represents a relatively small percentage of the total possible power savings. Even for the DPSK algorithm, a 0.35 dB margin exists between theoretical coherent detection.

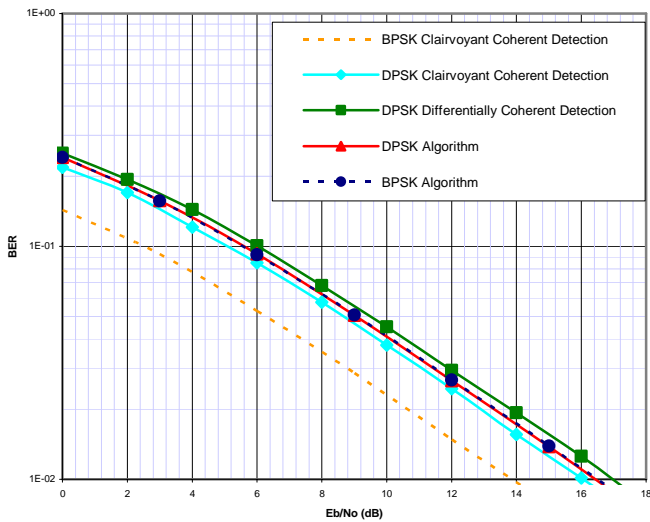


Figure 8: Slow Fading Channel - 1 Reference Symbol and 8 Information Symbols

In the AWGN and fast fading channels, the underperformance of the BPSK algorithm was the result of poor phase correction with one reference symbol. However, the results in Figure 9 demonstrate that with improved phase correction using two reference symbols, the BPSK algorithm was unable to achieve near theoretical performance in the slow fading environment. Even though this algorithm experienced an improved performance advantage of 1.75 dB over noncoherent DPSK detection, a considerable 1.40 dB difference remains between theoretical coherent detection. In contrast to the first two channels, the remaining difference was the consequence of phase errors uniformly distributed between  $\pm 90^\circ$  and  $\pm 180^\circ$ .

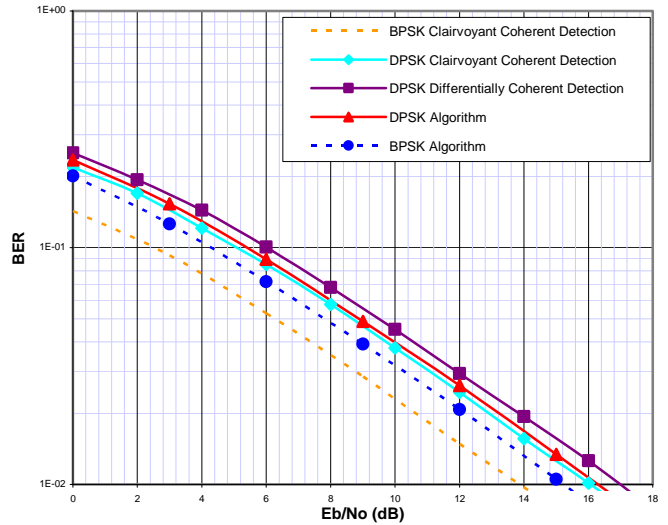


Figure 9: Slow Fading Channel - 2 Reference Symbols and 16 Information Symbols

## 4. FUTURE RESEARCH

The basic phase estimation squaring technique presented in this paper can be extended to QPSK and 8PSK modulated waveforms. Algorithm structures for these modulations are shown in Figures 10 and 11 (signal constellations?). Currently, the performance of these algorithms is being investigated in the three channels discussed in this paper.

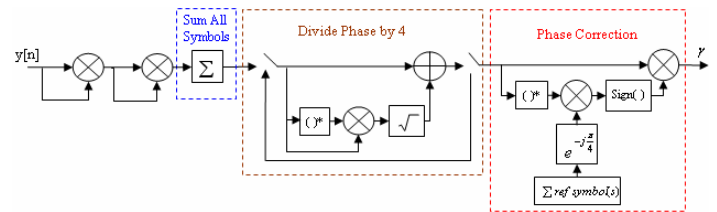


Figure 10: Block Diagram for QPSK Phase Estimation Algorithm

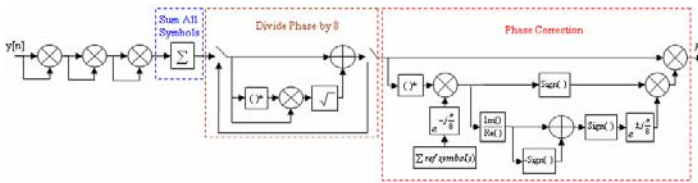


Figure 11: Block Diagram for 8PSK Phase Estimation Algorithm

## 5. CONCLUSION

This paper presented a unique approach to phase estimation that minimizes the power loss of binary PSK waveforms containing a small number of reference symbols. It was shown that in the three channels discussed, both the DPSK and BPSK algorithms performed more efficiently than differential phase modulations with noncoherent detection when hops contained only one reference symbol. Also, it was shown that when an additional reference symbol was added to each hop, the BPSK algorithm achieved significant power savings of up to 3 dB. Currently, we are investigating whether these performance gains can be realized when the algorithm is extended to QPSK and 8PSK modulations.

## 6. REFERENCES

- [1] J. G. Proakis, *Digital Communications*. New York: McGraw-Hill, 1983.
- [2] A. Papoulis, *Probability, Random Variables, and Stochastic Processes*. New York: McGraw-Hill, 1965.